Morphology Changes of Transition-Metal-Substituted Aluminophosphate Molecular Sieve $AlPO_4$-5 Crystals

Dayong Tian, Wenfu Yan, Xuejing Cao, Jihong Yu,* and Ruren Xu

State Key Laboratory of Inorganic Synthesis and Preparative Chemistry, College of Chemistry, Jilin University, Changchun 130012, P. R. China

Received November 21, 2007. Revised Manuscript Received January 15, 2008

In this work, poly ethylene glycol (pEG) was used as a cosolvent to control the morphology of transition metal substituted aluminophosphate molecular sieve $AlPO_4$-5 (AFI) crystals in the solvothermal reaction system of $Al(OPr^i)_3$-H_3PO_4-TEA-Me-H_2O-pEG (Me = Cr, Ti, Fe, V). In the presence of pEG molecules, the growth rate of the Me-AFI crystals along *c*-direction was significantly inhibited. With the increase of the volume ratio of pEG/H_2O, the aspect ratio of hexagonal prismlike Cr-AFI crystals was gradually decreased and the tabletlike crystals were obtained. Further increasing the volume ratio of pEG/H_2O resulted in the novel flowerlike morphology for Cr^{3+}- and Fe^{3+}-substituted AFI crystals and kiwi-fruit-like morphology for Ti^{4+} and V^{5+} substituted AFI crystals. Our studies revealed that the existence of pEG molecules and the isomorphic substitution of Al or P are important for the formation of these specific morphologies.

Introduction

Zeolites and aluminophosphate molecular sieves ($AlPO_4$-*n*), which have periodic three-dimensional framework and well-defined pore structures, have attracted much interest due to their wide applications in catalysis, ion-exchange, chemical separation, adsorption, host/guest chemistry, microelectronic devices, optics, and membranes.[1–3] Studies show that their special properties and applications are strongly affected by the morphology of the crystals.[4–10] For example, the diffusion of guest molecules in micropores and the catalytic adsorption performance of zeolite materials are strongly affected by the particle's morphology.[4] Therefore, the development of new synthetic strategies for controlling the crystal morphology of zeolite materials is becoming increasingly important.

In the past decades, several methods have been developed for the morphology control of zeolites and related microporous materials. In some cases, the crystal shape and size of zeolites can be manipulated by systematic variation of the synthetic parameters. For example, the aspect ratio (*b*/*c*) of mordenite crystals can be significantly reduced by increasing the alkalinity of the reaction system;[11] the size and shape of ETS-4 crystals can be modified by varying pH and the Na/K ratio of the synthetic gel.[12] In addition, the nature of structure-directing agents (SDAs) has been found to have influence on the morphology of zeolites.[13] Studies by Tsapatsis and co-workers revealed that dimmers and trimers of tetrapropylammonium hydroxide (TPAOH, SDA of silicalite-1) can drastically affect the morphology of silicalite-1 crystals.[14] Recently, Slater and co-workers developed a computational approach to investigate the influence of SDA on the growth of different crystal faces and their potential use on morphology control of zeolite crystals.[15] Their results suggest that TPAOH will preferentially be adsorbed onto (100) rather than the (010) surface of silicalite-1 crystal and further affect the relative growth rate of the corresponding crystallographic direction. Furthermore, Yoon and co-workers reported that adding inorganic additives such as LiCl and $MgCl_2$ in the reaction system can lead to a significant decrease in size of zeolite L.[6] On the other hand, synthesis in confined spaces, such as reverse micells, microemulsions and hydrogels, has been successfully employed to control the particle size and shape of zeolite crystals.[16–22]

* Corresponding author. E-mail: jihong@jlu.edu.cn. Fax: 86 431-8516-8608.

(1) Pool, R. *Science* **1994**, *263*, 1698.
(2) Davis, M. E. *Nature* **2002**, *417*, 813.
(3) Corma, A. *Chem. Rev.* **1997**, *97*, 2373.
(4) Drews, T. O.; Tsapatsis, M. *Curr. Opin. Colloid Interface Sci.* **2005**, *10*, 233.
(5) Lee, S.; Shin, C.; Hong, S. B. *J. Catal.* **2004**, *223*, 200.
(6) Lee, Y.; Lee, J. S.; Yoon, K. B. *Microporous Mesoporous Mater.* **2005**, *80*, 237.
(7) Li, S. A.; Li, Z. J.; Bozhilov, K. N.; Chen, Z. W.; Yan, Y. S. *J. Am. Chem. Soc.* **2004**, *126*, 10732.
(8) Lai, Z. P.; Bonilla, G.; Diaz, I.; Nery, J. G.; Sujaoti, K.; Amat, M. A.; Kokkoli, E.; Terasaki, O.; Thompson, R. W.; Tsapatsis, M.; Vlachos, D. G. *Science* **2003**, *300*, 456.
(9) Alsyouri, H. M.; Lin, J. Y. S. *J. Phys. Chem. B* **2005**, *109*, 13623.
(10) Chaikittisilp, W.; Davis, M. E.; Okubo, T. *Chem. Mater.* **2007**, *19*, 4120.
(11) Hamidi, F.; Bengueddach, A.; Di Renzo, F.; Fajula, F. *Catal. Lett.* **2003**, *87*, 149.
(12) Yilmaz, B.; Warzywoda, J.; Sacco, A., Jr. *J. Cryst. Growth* **2004**, *271*, 325.
(13) de Vos Burchart, E.; Jansen, J. C.; van de Graaf, B.; van Bekkum, H. *Zeolites* **1993**, *13*, 216.
(14) Bonilla, G.; Diaz, I.; Tsapatsis, M.; Jeong, H.; Lee, Y.; Vlachos, D. G. *Chem. Mater.* **2004**, *16*, 5697.
(15) Jelfs, K. E.; Slater, B.; Lewis, D. W.; Willock, D. J. *Stud. Surf. Sci. Catal.* **2007**, *170B*, 1685.
(16) Yates, M. Z.; Ott, K. C.; Birnbaum, E. R.; McCleskey, T. M. *Angew. Chem., Int. Ed.* **2002**, *41*, 476.
(17) Lin, J. C.; Dipre, J. T.; Yates, M. Z. *Chem. Mater.* **2003**, *15*, 2764.
(18) Lin, J. C.; Yates, M. Z. *Langmuir* **2005**, *21*, 2117.
(19) Lin, J. C.; Dipre, J. T.; Yates, M. Z. *Langmuir* **2004**, *20*, 1039.

10.1021/cm703317c CCC: $40.75
Published on Web 03/04/2008

Basically, the morphology of a crystal is determined by the growth rate of the crystal faces which have different surface energies during the crystallization.[23,24] Adding organic or inorganic additives in the reaction system can change the relative surface energies of different crystal faces and thus modify the morphology of the resulting crystal.[25,26] Herein, we describe a feasible approach to control the morphology of transition-metal-substituted aluminophosphate molecular sieve $AlPO_4$-5 (Me-AFI) via introduction of poly ethylene glycol molecules as a cosolvent that can inhibit the growth of the *c*-direction of AFI crystals.

$AlPO_4$-5 is one of the most famous members in the family of aluminophosphate molecular sieves.[27,28] Transition-metal-substituted $AlPO_4$-5 with active catalytic sites has been found important application in catalysis.[2,29,30] Poly ethylene glycol (pEG) is an important precursor for the preparation of many surfactants, which has good emulsification and lubrication ability. Recently, the derivative of pEG such as pEG-b-pGlu has been used in biomineralization process to control the growth of $CaCO_3$ by varying the mineral solubility, precipitation kinetics and solution properties.[31] In this work, the effect of pEG molecules on the growth of Me-AFI crystals has been investigated. The results demonstrate that the presence of pEG molecules can effectively inhibit the growth of the *c*-direction of AFI crystals. The volume ratio of pEG/H_2O in the reaction system has significant influence on the morphology of the Me-AFI crystals depending on the different isomorphic substitution mechanisms of transition metal ions. This new synthetic strategy may be applied to the control of the crystal morphology of other zeolites and related materials.

Experimental Section

Me-AFI (Me = Cr, Ti, Fe, V) crystals were synthesized from the reaction mixture of $Al(OPr^i)_3$-H_3PO_4-TEA-Me-H_2O-pEG at 180 °C. Reagents were used as received without further purification: aluminum triisopropoxide, phosphoric acid (85 wt % in water), triethylamine (TEA), chromium trichloride, tetrabutyl titanate, poly ethylene glycol 400 (molecular weight is 380–420), deionized water.

Synthesis of Tabletlike Cr-AFI Crystals. Typically, 0.5 g of well-ground aluminum triisopropoxide was first dispersed into 10 mL of mixed-solvents (pEG, 5 mL; H_2O, 5 mL) with stirring, followed by successive addition of 0.215 mL of phosphoric acid and 0.273 mL of triethylamine. Finally, 0.0391 g of $CrCl_3 \cdot 6H_2O$ was added to the above gel. The reaction gel with the molar composition of $Al(OPr^i)_3/1.3H_3PO_4/0.8TEA/0.06CrCl_3/113.4H_2O$ (the volume ratio of pEG/H_2O was 1/1) was further stirred for 12 h at ambient temperature and was then sealed in a Teflon-lined stainless steel autoclave and heated at 180 °C for 12 h under static conditions. The solid product was filtrated, washed with distilled water, and dried at 50 °C overnight.

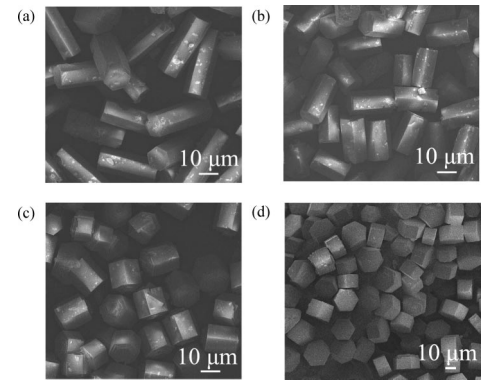

Figure 1. SEM images of the Cr-AFI crystals with different aspect ratios obtained in the reaction systems with different volume ratios of pEG/H_2O: (a) pEG:H_2O = 1:4; (b) pEG:H_2O = 3:7; (c) pEG:H_2O = 2:3; (d) pEG:H_2O = 1:1. The total volume of pEG and H_2O is 10 mL.

Synthesis of Flowerlike Cr-AFI Crystals and Kiwi-Fruit-Like Ti-AFI Crystals. Typically, 0.3 g of well-ground aluminum triisopropoxide was first dispersed into 10 mL of mixed solvent (pEG, 7 mL; H_2O, 3 mL) with stirring, followed by successive addition of 0.129 mL of phosphoric acid and 0.164 mL of triethylamine. Finally, 0.0196 g of $CrCl_3 \cdot 6H_2O$ or 0.035 mL of tetrabutyl titanate was added to the above gel to give a final gel with molar composition of $Al(OPr^i)_3/1.3H_3PO_4/0.8TEA/0.05CrCl_3$ or $[0.07(C_4H_9O)_4Ti]/113.4H_2O$ (the volume ratio of pEG/H_2O was 7/3). The reaction gel was further stirred for 12 h at ambient temperature, and sealed in a Teflon-lined stainless steel autoclave, and then heated at 180 °C for 24 h under static conditions. The solid product was filtrated, washed with distilled water, and dried at 50 °C overnight.

Characterization. X-ray powder diffraction (XRD) patterns were recorded on a Siemens D5005 diffractometer with Cu Kα (λ = 1.5418 Å) radiation. The crystal morphology was studied by field-emission scanning electron microscopy (JEOL JSM-6700F) using conventional sample preparation and imaging techniques. The diffuse reflectance UV–vis spectra were obtained on a Perkin-Elmer Lambda-20 spectrometer.

Results and Discussion

Synthesis of Cr-AFI Crystals. In the mixed-solvents system of pEG and H_2O, the pEG/H_2O volume ratio was found to have important influence on the resulting morphology of AFI crystals. The hexagonal prismlike Cr-AFI crystals, typical for AFI, were synthesized from the reaction system with the molar composition of $Al(OPr^i)_3/1.3H_3PO_4/0.8TEA/0.06CrCl_3/181.4H_2O$ (the volume ratio of pEG/H_2O is 1/4). Figure 1a shows the SEM image of as-synthesized Cr-AFI crystals. Increasing the volume ratio of pEG/H_2O resulted in the decrease of the aspect ratio of Cr-AFI crystals (images b and c in Figure 1). When the volume ratio of pEG/H_2O was increased to 1/1, the tabletlike crystals were obtained (Figure 1d), which indicated that the growth rate of the Cr-AFI crystals along *c*-direction was inhibited by the pEG molecules. Accordingly, the average aspect ratio of the crystals shown in Figure 1a−d decreased from 3.0 to 0.7. Further increasing the pEG content, i.e., the volume ratio

(20) Lee, S.; Shantz, D. F. *Chem. Commun.* **2004**, 680.
(21) Dutta, P. K.; Jakupca, M.; Narayana, K. S.; Salvati, L. *Nature* **1995**, *374*, 44.
(22) Wang, H.; Holmberg, B. A.; Yan, Y. *J. Am. Chem. Soc.* **2003**, *125*, 9928.
(23) Mullin, J. W. *Crystallization*; Butterworths: London, 1971.
(24) Buckley, H. E. *Crystal Growth*; Wiley: New York, 1951.
(25) Mann, S. *Angew. Chem., Int. Ed.* **2000**, *39*, 3392.
(26) Adair, J.; Suvaci, H. E. *Curr. Opin. Colloid Interface Sci.* **2000**, *5*, 160.
(27) Wilson, S. T.; Lok, B. M.; Messian, C. A.; Cannan, T. R.; Flanigen, E. M. *J. Am. Chem. Soc.* **1982**, *104*, 1146.
(28) Yu, J.; Xu, R. *Acc. Chem. Res.* **2003**, *36*, 481.
(29) Hartmann, M.; Kevan, L. *Chem. Rev.* **1999**, *99*, 635.
(30) Thomas, J. M.; Raja, R.; Sankar, G.; Bell, R. G. *Acc. Chem. Res.* **2001**, *34*, 191.
(31) Guo, X. H.; Yu, S. H.; Cai, G. B. *Angew. Chem., Int. Ed.* **2006**, *45*, 3977.

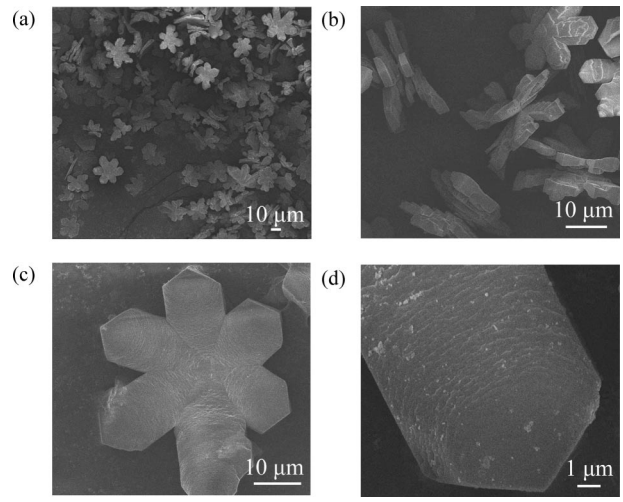

Figure 2. SEM images of the flowerlike Cr-AFI crystals obtained in the mixed-solvents system of pEG and H_2O: (a) a large scale of the product at a low magnification; (b) the flank image of the double-fold flowerlike Cr-AFI crystals; (c) a single flowerlike Cr-AFI crystal viewed from the top perspective at a high magnification; (d) the cleaved terraces on the surface of one petal.

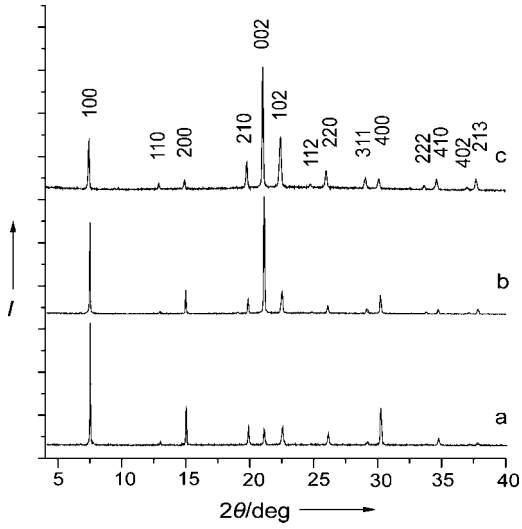

Figure 3. XRD patterns of the Cr-AFI crystals with different morphologies: (a) prismlike crystals; (b) tabletlike crystals; (c) flowerlike crystals.

of pEG/H_2O reached 7/3, novel self-supported double-fold hexagonal flowerlike Cr-AFI crystals were obtained (Figure 2a and b). Figure 2c shows the high-magnification SEM image of one hexagonal flowerlike crystal viewed from the top perspective. The hexagonal flowerlike crystal has six petals extending radially from the center of the hexagonal flower. The high-magnification SEM image reveals the cleavage nature of the surface of the petal (Figure 2d). An array of terraces can be found on the surface.

Figure 3 shows the X-ray powder diffraction (XRD) patterns of as-prepared Cr-AFI crystals shown in Figure 1a, Figure 1d, and Figure 2a. The position of the diffraction peaks of all samples matches well with that of the simulated XRD pattern of AFI framework.[32] However, the relative intensities of the diffraction peak of crystal face (002) of the flowerlike and tabletlike crystals are much higher than that of the prismlike crystals, which agrees well with the fact that the former crystals have much lower aspect ratio.

Previously, Klap and co-workers studied the polar growth of large $AlPO_4$-5 crystals with scanning pyroelectric microscopy and found a sharp reversal of the pyroelectric activity in the midplane of the crystals, which indicated that the polarization reversed at the center of the crystal and suggested that the crystals were twinned.[33] Their study by polar molecules entering the pores of the crystal revealed that the external surfaces of (001) face consisted of Al atoms. At these surfaces the Al atom is probably four-coordinated with an additional −OH group.[33,34] Furthermore, the terminal P atom exists in the form of P═O instead of P−OH. Therefore, the side faces that are terminated by alternate Al and P atoms may have more P═O groups which will result in a lower density of −OH groups in comparison to the (001) face.

In our work, the pEG molecules were added to the reaction system to modify the AFI crystal growth through the interactions with the chemically different surfaces of AFI crystals. In terms of the experimental results that increasing the volume ratio of pEG/H_2O can lead to the increased inhibition effect on the crystal growth along *c*-direction, the interaction of pEG with the (001) face appears to be stronger compared with the side faces. With further increasing the volume ratio of pEG/H_2O, the growth rate along the *c*-axis was significantly inhibited, whereas the growth rate along other directions was relatively weakened, which resulted in the novel flowerlike crystal shape. Therefore, we propose that the pEG molecules may play a site specific role which can drastically decrease the surface energy of the (001) face than the side faces in the interaction with the different surfaces of AFI crystals. The role of Cr^{3+} ions in the formation of this flowerlike crystal shape is not well understood yet. However, without the Cr^{3+} ions in the reaction system, the regular hexagonal flowerlike crystals can not be obtained (see the Supporting Information, Figure S1). Therefore, the Cr^{3+} ions favor the formation of regular flowerlike Cr-AFI crystals.

Synthesis of Ti-AFI Crystals. To study the influence of pEG molecule on the morphology of other Me-AFI crystals, $Ti^{4+}$was added into the reaction system, whereas other experiment conditions were kept the same as those for the synthesis of flowerlike Cr-AFI crystals. Interestingly, the Ti-AFI microspheres with kiwi fruit morphology as shown in Figure 4 were obtained. The AFI nature of these kiwi-fruit-like microspheres was confirmed by the XRD analysis (see the Supporting Information, Figure S2). Figure 4a shows the SEM image of the kiwi-fruit-like microspheres at low magnification that exhibit excellent monodispersity. The inset of Figure 4a shows the top view of a typical kiwi-fruit-like Ti-AFI microsphere. Two small cavities with the diameter of about 1–2 μm were found on the top and bottom of the microsphere. Figure 4b shows the side view of such kiwi-fruit-like Ti-AFI microsphere. High-magnification SEM

(32) Treacy, M. M.; Higgins, J. J. B.; von Ballmoos, R. *Collection of Simulated XRD Powder Patterns for Zeolites*; Elsevier: New York, 1996, 352.

(33) Klap, G. J.; Wubbenhorst, M.; Jansen, J. C.; van Koningsveld, H.; van Bekkum, H.; van Turnhout, J. *Chem. Mater.* **1999**, *11*, 3497.

(34) Klap, G. J.; van Klooster, S. M.; Wubbenhorst, M.; Jansen, J. C.; van Bekkum, H.; van Turnhout, J. *J. Phys. Chem. B* **1998**, *102*, 9518.

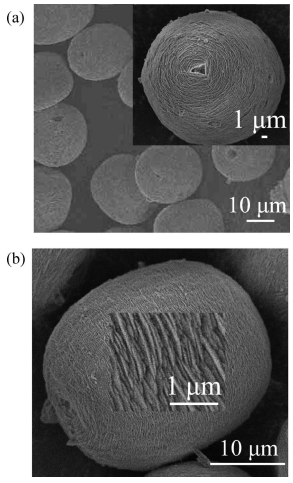

Figure 4. SEM images of the kiwi-fruit-like Ti-AFI crystals: (a) a large scale of the product at a low magnification, the inset is a top image of the crystal; (b) a flank image of the crystal, the inset is a high-magnification image of the flank surface, which is composed of compact sheetlike crystals stacking together.

image of the surface (inset of Figure 4b) suggests that this Ti-AFI microsphere consists of small compact sheets with the thickness of several tens nanometers.

To further investigate the formation of these Ti-AFI microspheres, the products produced at different growth stages were studied in detail using SEM analysis. By crystallization of the reactants for different reaction times, partially formed kiwi-fruit-like microsphere intermediates throughout the growth process can be obtained. Figure 5a−d shows the evolution process of the intermediates. At the first stage, columniform structure was formed (Figure 5a), which is composed of ultra thin sheets with nanoscale thickness (Figure 5a′). With prolonging the reaction time, the formation of the sheetlike crystals prefers to take place at the peripheral parts which resulted in a concave on the surface of the intermediates (images b and c in Figure 5). Figure 5b′−d′ shows the top magnification images of the intermediates at different successive growth stages, revealing the stacking fashion of the sheetlike nanocrystals. The sheets on the peripheral parts were continuously formed, whereas the sheet formation on the inside part appeared to be inhibited, resulting in the oncoming formed sheets stacking with a progressively tilted angle and further forming a cavity at the end of the crystallization (Figure 5d). The concave feature in the growth process can be explained thermodynamically that the concave surface has a much lower surface energy than the convex surface for a given material.[35] These results demonstrate that the kiwi-fruit-like microsphere is a superstructure made by highly crystallized and controlled aligned Ti-AFI microcrystals. The formation of the ultra thin sheetlike Ti-AFI crystals indicates the growth of AFI along *c*-direction is dramatically inhibited due to the synergetic effect of Ti ions and the pEG molecules.

Isomorphic Substitutions of Me-AFI. As described above, Cr^{3+} and Ti^{4+} substituted AFI crystals show completely different morphologies. However, their experimental crystallization conditions are almost same except for the different

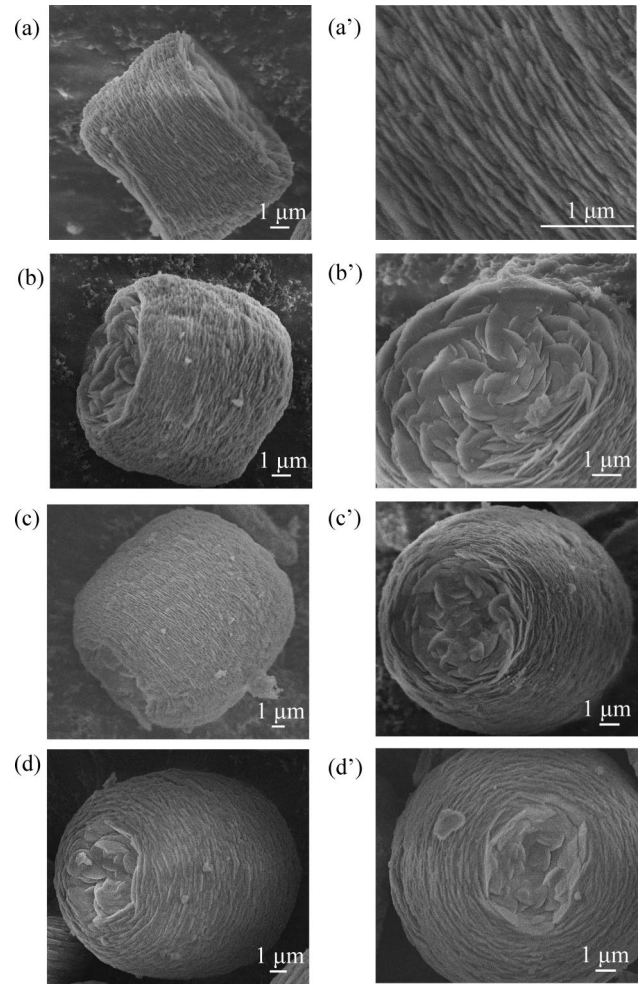

Figure 5. From (a) to (d): SEM images of the Ti-AFI crystal taken at different growth stages. (a′) High-magnification SEM image of (a). From (b′) to (d′): the SEM images of the top view of the Ti-AFI crystal at different growth stages.

types of transition metal ions. In both cases, pEG acts as a crystal growth inhibitor. Thus, the different isomorphic substitutions may account for the different morphologies of AFI crystals formed in the presence of pEG. The UV–vis adsorption was measured for Cr and Ti-AFI samples. UV–vis spectrum of the flowerlike Cr-AFI, along with the prismlike and tabletlike Cr-AFI samples, shows adsorption bands at 290, 440, and 620 nm (Figure 6), which are generally assigned to $^4A_{2g}(F) \rightarrow {}^4T_{1g}(P)$, $^4A_{2g}(F) \rightarrow {}^4T_{1g}(F)$, and $^4A_{2g}(F) \rightarrow {}^4T_{2g}(F)$ transitions, respectively.[36] These bands are characteristic for a stable framework substitution of Cr^{3+} in distorted octahedral coordination (Cr^{3+} is 4-fold bonded to the framework and the coordination is complemented by water molecules in pores).[37] UV–vis spectrum of Ti-AFI sample shows a maximum at 240 nm that can be assigned to ligand-to-metal charge-transfer transition between oxygen and tetracoordinated Ti^{4+} ions (Figure 7),[38,39] which indicates that Ti^{4+} is incorporated into the framework of AFI.

(35) Ghoshal, T.; Kar, S.; Chaudhuri, S. *Cryst. Growth Des.* **2007**, *7*, 136.
(36) Weckhuysen, B. M.; De Ridder, L. M.; Schoonheydt, R. A. *J. Phys. Chem. B* **1993**, *97*, 4756.
(37) Kornatowski, J.; Zadrozna, G.; Rozwadowski, M.; Zibrowius, B.; Marlow, F.; Lercher, J. A. *Chem. Mater.* **2001**, *13*, 4447.
(38) Chang, Z. X.; Koodali, R.; Krishna, R. M.; Kevan, L. *J. Phys. Chem. B* **2000**, *104*, 5579.
(39) Prakash, A. M.; Kevan, L.; Zahedi-Niaki, M. H.; Kaliaguine, S. *J. Phys. Chem. B* **1999**, *103*, 831.

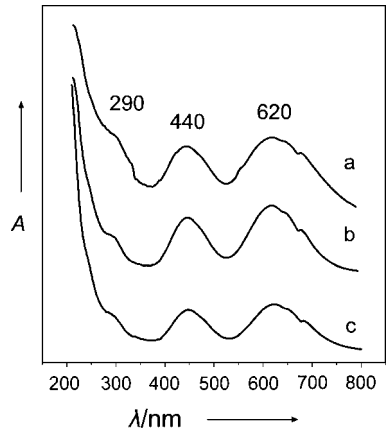

Figure 6. UV–vis diffuse reflectance spectra of Cr-AFI: (a) prismlike crystals; (b) tabletlike crystals; (c) flowerlike crystals.

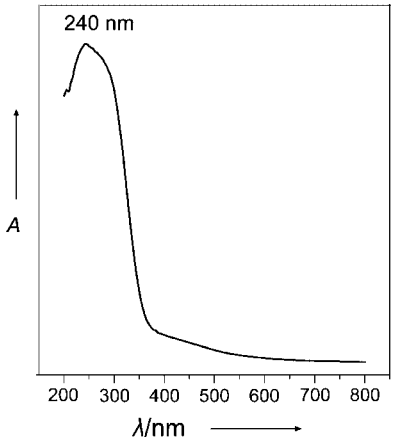

Figure 7. UV–vis diffuse reflectance spectrum of Ti-AFI.

As is known, the isomorphic substitution mechanisms for aluminophosphates can be classified into substitution of Al atoms, substitution of P atoms, and substitution of pairs of adjacent Al and P atoms, depending the valence and radius of the substituted cations.[40] Accordingly, in the transition-metal-substituted aluminophosphate framework, Cr^{3+} and Ti^{4+} will substitute Al atoms and P atoms, respectively.[41,42] In the presence of pEG molecules, the introduction of Cr^{3+} into the framework leads to the hexagonal double-fold flowerlike crystals, while the introduction of Ti^{4+} into the framework results in the kiwi fruit shape of the crystals. Therefore, the different isomorphic substitution mechanisms of transition metal ions in AFI may be responsible for the different growth behavior of the Me-AFI crystals with the presence of pEG molecules in the reaction system. Furthermore, other transition metal ions such as Fe^{3+} and V^{5+} were added into the reaction system, respectively. Accordingly, the imperfect hexagonal flowerlike Fe-AFI crystals (with the similar substituted mechanism of Cr^{3+}) and the kiwi-fruit-like V-AFI crystals (with the similar substituted mechanism of Ti^{4+}) were obtained (see the Supporting Information, Figure S3). These results indicate that the different metal ions may also affect the crystallization kinetic depending on the isomorphic substitution mechanism of AFI crystals.

Conclusions

In this work, the pEG has been used as a cosolvent to control the crystal growth of transition-metal-substituted AFI crystals. The results demonstrate that the crystal growth of AFI crystal along *c*-axis can be significantly inhibited by using pEG molecules as the crystal growth inhibitor. Varying the volume ratio of pEG/H_2O, different morphologies of AFI crystals can be obtained, such as prismlike, tabletlike, and flowerlike Cr-AFI, and kiwi-fruit-like Ti-AFI crystals depending on the type of transition metal ions in the reaction system. Our work suggests that the different isomorphic substitution of metal ions may be responsible for the different growth behavior of Me-AFI crystals with the presence of pEG in the reaction system. This work provides a new way for the controlled crystallization of metal-substituted aluminophosphate molecular sieves.

Acknowledgment. We acknowledge the special funding support from the National Natural Science Foundation of China and the State Basic Research Projects of China (2006CB806103 and 2007CB936402).

Supporting Information Available: SEM images of V- and Fe-AFI crystals; XRD patterns of Ti-, V- and Fe-AFI crystals (PDF). This material is available free of charge via the Internet at http://pubs.acs.org.

CM703317C

(40) Martens, J. A.; Jacobs, P. A. *Stud. Surf. Sci. Catal.* **1994**, *85*, 653.
(41) Helliwell, M.; Kaucic, V.; Cheetham, G. M. T.; Harding, M. M.; Kariuki, B. M.; Rizkallah, P. J. *Acta Crystallogr., Sect. B* **1993**, *49*, 413.
(42) Prakash, A. M.; Kurshev, V.; Kevan, L. *J. Phys. Chem. B* **1997**, *101*, 9794.